






ORIGINAL RESEARCH

Somatic Mosaicism of a PDGFRB Activating Variant in Aneurysms of the Intracranial, Coronary, Aortic, and Radial Artery Vascular Beds

Carolina A. Parada, PhD*; Fatima M. El-Ghazali, BS*; Daphne Togliola, BS*; Jacob Ruzevick, MD; Malia McAvoy, MD; Samuel Emerson, MD, PhD; Yigit Karasozen, MD; Tina Busald, BS; Ahmad A. Nazem , PhD; Shaun M. Suranowitz, BS; Sherene Shalhub , MD, MPH; Desiree A. Marshall , MD; Luis F. Gonzalez-Cuyar , MD; Michael O. Dorschner, PhD; Manuel Ferreira Jr.,  MD, PhD

BACKGROUND: Activating variants in platelet-derived growth factor receptor beta (PDGFRB), including a variant we have previously described (p.Tyr562Cys [g.149505130T>C [GRCh37/hg19]; c.1685A>G]), are associated with development of multiorgan pathology, including aneurysm formation. To investigate the association between the allele fraction genotype and histopathologic phenotype, we performed an expanded evaluation of post-mortem normal and aneurysmal tissue specimens from the previously published index patient.

METHODS AND RESULTS: Following death due to diffuse subarachnoid hemorrhage in a patient with mosaic expression of the above PDGFRB variant, specimens from the intracranial, coronary, radial and aortic arteries were harvested. DNA was extracted and alternate allele fractions (AAF) of *PDGFRB* were determined using digital droplet PCR. Radiographic and histopathologic findings, together with genotype expression of *PDGFRB* were then correlated in aneurysmal tissue and compared to non-aneurysmal tissue. The *PDGFRB* variant was identified in the vertebral artery, basilar artery, and P1 segment aneurysms (AAF: 28.7%, 16.4%, and 17.8%, respectively). It was also identified in the coronary and radial artery aneurysms (AAF: 22.3% and 20.6%, respectively). In phenotypically normal intracranial and coronary artery tissues, the *PDGFRB* variant was not present. The *PDGFRB* variant was absent from lymphocyte DNA and normal tissue, confirming it to be a non-germline somatic variant. Primary cell cultures from a radial artery aneurysm localized the *PDGFRB* variant to CD31-, non-endothelial cells.

CONCLUSIONS: Constitutive expression of PDGFRB within the arterial wall is associated with the development of human fusiform aneurysms. The role of targeted therapy with tyrosine kinase inhibitors in fusiform aneurysms with *PDGFRB* mutations should be further studied.

Key Words: cerebral aneurysm ■ fusiform ■ mosaic ■ PDGFRB

Platelet-derived growth factor receptor beta (PDGFRB) is a tyrosine kinase receptor involved in activation of multiple signaling pathways promoting cellular proliferation and survival.¹ Our group first described the role of a somatic activating variant

of *PDGFRB* in the formation of fusiform cerebral aneurysms.² We described a 23-year-old man with multiple enlarging fusiform intracranial aneurysms ipsilateral to a unique cutaneous phenotype. The phenotype was identified upon his initial presentation at 9 years of age for coil

Correspondence to: Manuel Ferreira, Jr., MD, PhD, University of Washington School of Medicine, Department of Neurological Surgery, 1959 NE Pacific St., Seattle, Washington. E-mail: manuelf3@uw.edu

*C. A. Parada, F. M. El-Ghazali, and D. Togliola contributed equally.

For Sources of Funding and Disclosures, see page 8.

© 2022 The Authors. Published on behalf of the American Heart Association, Inc., by Wiley. This is an open access article under the terms of the Creative Commons Attribution-NonCommercial License, which permits use, distribution and reproduction in any medium, provided the original work is properly cited and is not used for commercial purposes.

JAHA is available at: www.ahajournals.org/journal/jaha

CLINICAL PERSPECTIVE

What Is New?

- Fusiform aneurysms represent a challenging clinical entity with high potential for patient morbidity and death.
- A somatic activating variant of platelet-derived growth factor receptor beta (PDGFRB) is associated with the development of fusiform aneurysms.
- Mosaic expression of activated PDGFRB is associated with fusiform aneurysm development in various vascular territories.

What Are the Clinical Implications?

- PDGFRB represents a possible targetable mutation in patients with fusiform aneurysms.

Nonstandard Abbreviations and Acronyms

AAF	Alternate allele fraction
ddPCR	Digital droplet PCR
PAVS	platelet-derived growth factor receptor beta activating disorder
PDGFRB	platelet-derived growth factor receptor beta

embolization of a right internal carotid artery dissecting fusiform aneurysm. Despite negative cranial imaging for additional aneurysms at the time of presentation, he returned 12 years later for surgical repair of a dissecting ipsilateral fusiform intracranial vertebral artery aneurysm and later repair of a coronary artery aneurysm. DNA analyses revealed a somatic mosaic pattern of a *PDGFRB* variant within the aneurysmal tissue that was not present in grossly and histologically normal specimens or blood.

Both germline and somatic mosaicism represent mechanisms for genetic heterogeneity within an individual and is a result of the fidelity of DNA replication. Somatic mosaicism is a result of post-zygotic mutations leading to unique cell lineages. While many somatic cells containing errors in genetic replication undergo negative selection, those which escape such negative selection are implicated in a spectrum of human pathologies, including vascular disease.³

PDGFRB is expressed by perivascular mesenchymal cells and is particularly important for blood vessel formation.^{1,4,5} Gain of function variants of *PDGFRB* have been implicated in cancer, vascular pathology, and multiple syndromes with overlapping phenotypes including infantile myofibromatosis, Kosaki overgrowth

syndrome, and Penttinen premature aging syndrome.^{6–10} However, its role in the development of fusiform aneurysms has only recently been established.^{2,11}

The index patient died at the age of 29 due to diffuse subarachnoid hemorrhage secondary to a ruptured basilar artery aneurysm following publication of our initial manuscript. Given the clear pattern of aneurysmal development within multiple vascular territories, we aimed to investigate the association between the alternate allele fractions (AAF) of his activating *PDGFRB* variant and the histopathologic phenotype in an expanded evaluation of 80 post-mortem tissue specimens.

METHODS

The data that support this study are available from the senior author upon reasonable request.

Human Subject

Case study of the index individual, as described previously, was completed with the goal of further characterizing a previously identified activating *PDGFRB* variant (p. Tyr562Cys [g.149505130T>C [GRCh37/hg19]; c.1685A>G]) displaying somatic mosaicism and correlating its role in the pathogenesis of fusiform aneurysms. The pathologic phenotype based on gross anatomy, radiographic imaging, and microscopic histology was compared to *PDGFRB* allelic genotype using deep targeted sequencing methods. Premortem and postmortem tissue specimens were included from the patient's aneurysms, normal vasculature, and blood. All tissue specimens studied were obtained with appropriate consent and all protocols were reviewed and approved by the University of Washington institutional human subjects review board.

Tissue Specimen Collection & Preservation

Premortem aneurysmal repair operations were performed by the surgical teams at the University of Washington affiliated hospitals. The cerebral vasculature and aortic tissue were preserved using flash frozen paraffin embedded (FFPE) technique. Radial artery, saphenous vein, and coronary arteries were preserved using both FFPE and fresh frozen technique. Elective donation of the patient's body was completed per family's request under the supervision of a board-certified forensic pathologist and neuropathologist (DAM) and a board-certified neuropathologist (LFGC). Autopsy was completed within 16 hours of death.

Cell Cultures

Premortem specimens from skin, radial artery aneurysm, and saphenous vein were processed to establish primary cell lines from the index individual. The

endothelial, CD31 positive, cell population was isolated using Dynabeads CD31 Endothelial Cell Beads (Invitrogen) for all primary cell cultures.

Histology and H&E Staining

Hematoxylin & Eosin, Gomori's trichrome, and Verhoeff's-Van Gieson staining was completed for all samples. Histologic analysis was performed in a single-blinded fashion by board-certified neuropathologists (D.A.M. and L.F.G.C.).

DNA Extraction and Digital Droplet PCR

DNA was extracted from both frozen and FFPE tissue samples taken at autopsy. DNA was also extracted from primary cell pellets. DNA extractions on FFPE tissue samples were conducted with the QS GeneRead DNA FFPE (Qiagen) treatment protocol with modifications. A DNA repair step using the NEBNext FFPE DNA Repair Mix (New England Biolabs) was performed to ensure the integrity of both DNA and RNA available from FFPE tissue. Ten nanograms of DNA was used per digital droplet PCR (ddPCR) reaction, using previously described methods.^{12,13} Four independent replicates were performed on each tissue. Mutant (FAM) and wild-type (HEX) droplet thresholds were established using positive and negative controls included in each run: positive genomic control (35%), negative genomic control, and a no-template control. Multiple wells containing independent replicates were merged for analysis and Poisson CIs were defined using Quantasoft software (Bio-Rad, Hercules, CA Version 1.7). Those with <10 000 total droplets were excluded based on established guidelines.

Statistical Analysis

QuantaSoft parameters were set based on oligonucleotide control thresholds. Droplets were deemed positive for the *PDGFRB* variant if they fell within the established thresholds. AAF of the *PDGFRB* variant were calculated using the concentration of the mutant-positive droplets divided by the total amount of DNA-containing droplets (variant+wildtype droplets). AAFs were deemed positive under 2 conditions: the Poisson CIs of the mutant and wildtype droplets did not overlap and the AAF value fell within its own sample CIs. When the 95% CI overlapped that of the wildtype control, these samples were considered negative.¹⁴ All figures were created using RStudio (RStudio, Boston, MA, Version 1.4.1106).

RESULTS

Clinical Course

A 21-year-old man with a predominantly right-sided cutaneous phenotype presented for care at the

University of Washington Hospital health system, having previously undergone coil embolization of a right carotid fusiform aneurysm at the age of nine. Follow-up imaging revealed an unruptured right vertebral artery fusiform aneurysm as well as a right P1 segment posterior cerebral artery fusiform aneurysm. He underwent multiple endovascular and microsurgical operations for occlusion and bypass of the vertebral artery fusiform aneurysm. Six years later, he experienced palpitations leading to cardiac work-up where a 3.4×3.0×2.8 cm distal left main coronary artery aneurysm was discovered. He subsequently underwent cardiac stenting and bypass for exclusion of the aneurysm. Two years following this operation, at the age of 29, he underwent resection of an enlarging right radial artery aneurysm using a saphenous vein interposition graft. Tissue specimens were harvested at this time to establish primary cultures. Further cranial imaging revealed progression of the right P1 segment fusiform aneurysm and development of a mid-basilar fusiform aneurysm. Unfortunately, prior to treatment, he experienced rupture of the mid-basilar fusiform artery aneurysm with resultant subarachnoid and intraventricular hemorrhage leading to acute intracranial hypertension, causing death (Figure 1).

Intracranial Arteries

AAF from tissue of the intracranial circulation ranged from 0% to 28.7%, with higher AAF representing the presence of the *PDGFRB* variant and correlating with the identification of fusiform aneurysms. The *PDGFRB* variant was present in the right vertebral artery aneurysm (proximal and distal AAF: 17.5% and 28.7%, respectively), mid-basilar aneurysm (AAF: 16.4%), and right P1 segment aneurysms (AAF: 17.8%). The *PDGFRB* variant was also present in the tissue from the PCA, immediately adjacent to the P1 segment aneurysm (AAF: 21.1%). Comparatively, sites without obvious aneurysmal dilatations had lower AAFs. The AAF of the unaffected right carotid artery, the right anterior cerebral artery, and the left middle cerebral artery were 2.7%, 2.9%, and 4.3%, respectively.

The AAF of the unaffected right middle cerebral artery and left anterior cerebral artery sites was 0 and the Poisson CIs overlapped with the wildtype negative control suggesting a lack of expression of the *PDGFRB* variant. The AAF of the unaffected left common carotid artery was 0.3%. Its Poisson CI also overlapped with the negative control suggesting a lack of expression of the *PDGFRB* variant (Figure 2A).

Histopathological evaluation of the intracranial fusiform aneurysms showed proliferation of medial smooth muscle medial cells with haphazard arrangement and variable nuclear pleomorphism. There was marked

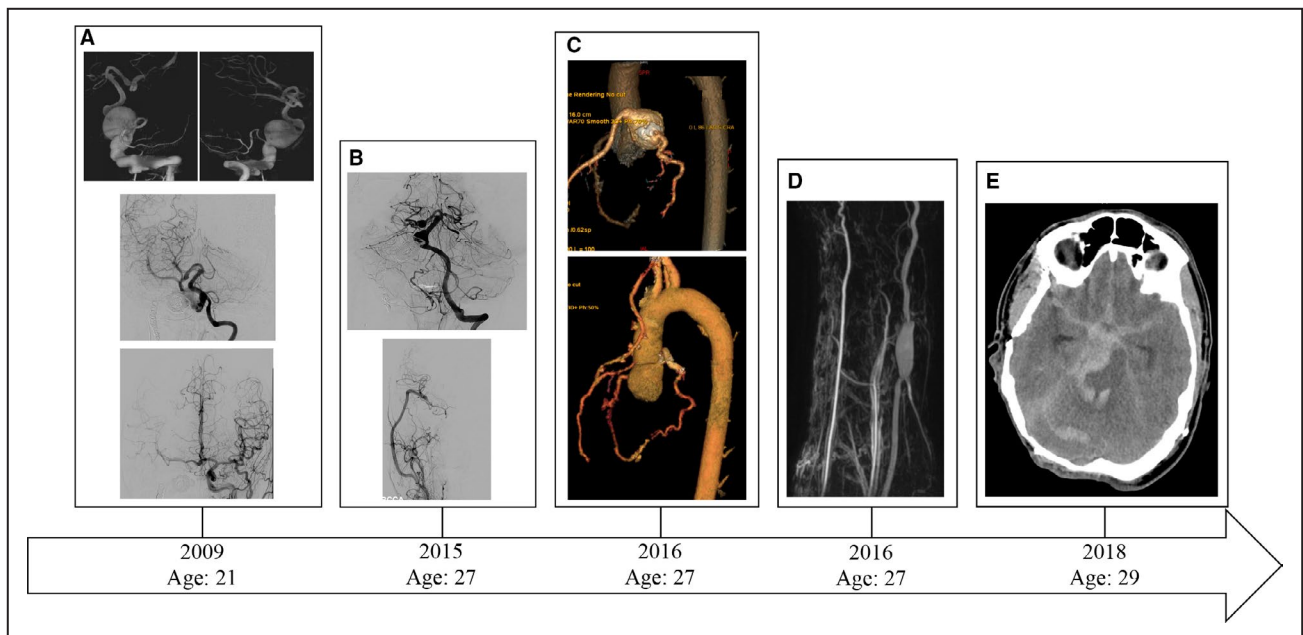


Figure 1. Radiographic correlate of the index patient's clinical course.

A, (Top row) Digital subtraction angiography showing 3D reconstruction of a right vertebral artery fusiform aneurysm after a right vertebral injection. A fusiform aneurysm encompassing the extracranial and intracranial vertebral artery is seen. (Middle) Post-treatment left vertebral artery injection shows a normal left vertebral artery and small fusiform dilatation of the right P1 segment. The right vertebral artery underwent coil embolization/sacrifice with bypass. (Bottom) Digital subtraction angiogram with Townes view of a left common carotid artery injection. The right anterior circulation is seen due to cross-filling via a patent anterior communicating artery. No aneurysmal pathology is identified in the anterior circulation. The right common carotid artery had previously undergone coil embolization and sacrifice. **B,** Follow-up digital subtraction angiography showing (Top) progression of the right P1 segment fusiform aneurysm as well as development of a mid-basilar artery aneurysm and (Bottom) right external carotid artery to middle cerebral artery bypass with normal right middle cerebral artery candelabra. **C,** (Top) Identification of a coronary artery aneurysm and (Bottom) post-treatment imaging. **D,** Identification of a right radial artery fusiform aneurysm. **E,** Non-contrast computed tomography showing diffuse subarachnoid hemorrhage secondary to a ruptured basilar artery aneurysm causing death.

fibrointimal proliferation with extensive effacement of the internal elastic lamina. In addition, there was adherent intraluminal thrombus in various stages of organization, including acute with fibrin layering, early organizing, and remote with fibrosis and neovascularization (Figure 3).

Coronary Arteries

Similar to the presence of the *PDGFRB* variant in the intracranial aneurysms, the *PDGFRB* variant was also identified in the coronary artery aneurysm. The AAF from aneurysmal tissue was 22.3%. In contrast the AAF of the proximal and distal left coronary artery was 0.28% and 0%, respectively. The Poisson CI of these non-aneurysmal samples overlapped with the wildtype negative control suggesting a lack of the *PDGFRB* variant.

Complete histopathological assessment of the coronary artery aneurysm was precluded due to structural alterations induced by the stenting procedure. However, nodular fibro-intimal proliferation with focal calcification and scattered ectatic vascular spaces were identified. The recognizable portions of peripheral

coronary vessel wall showed fascicular and haphazard medial proliferation with moderate hypercellularity. Focal proliferative regions with granulation tissue-like appearance, foamy and pigment laden macrophages, hemosiderin, and cholesterol clefts were present and suggestive of organizing thrombus (Figure 3).

Aorta

Multiple locations starting at the aortic root and extending to the distal abdominal aorta were sampled in pairs with one pair from each sample showing variable AAFs ranging from 0% to 35.1%. The entirety of the aortic wall was visualized and analyzed. CT angiography and gross anatomical examination by the team of pathologists did not reveal any obvious thoracic or abdominal aortic aneurysms. However, histopathological examination from the proximal aortic arch showed various degrees of pathological alterations consistent with microdissections at various stages of remodeling (Figure 3). One blinded pathologist reviewing these aortic samples was able to accurately rank the more affected sampled from higher to lower AAF based on histopathological features alone.

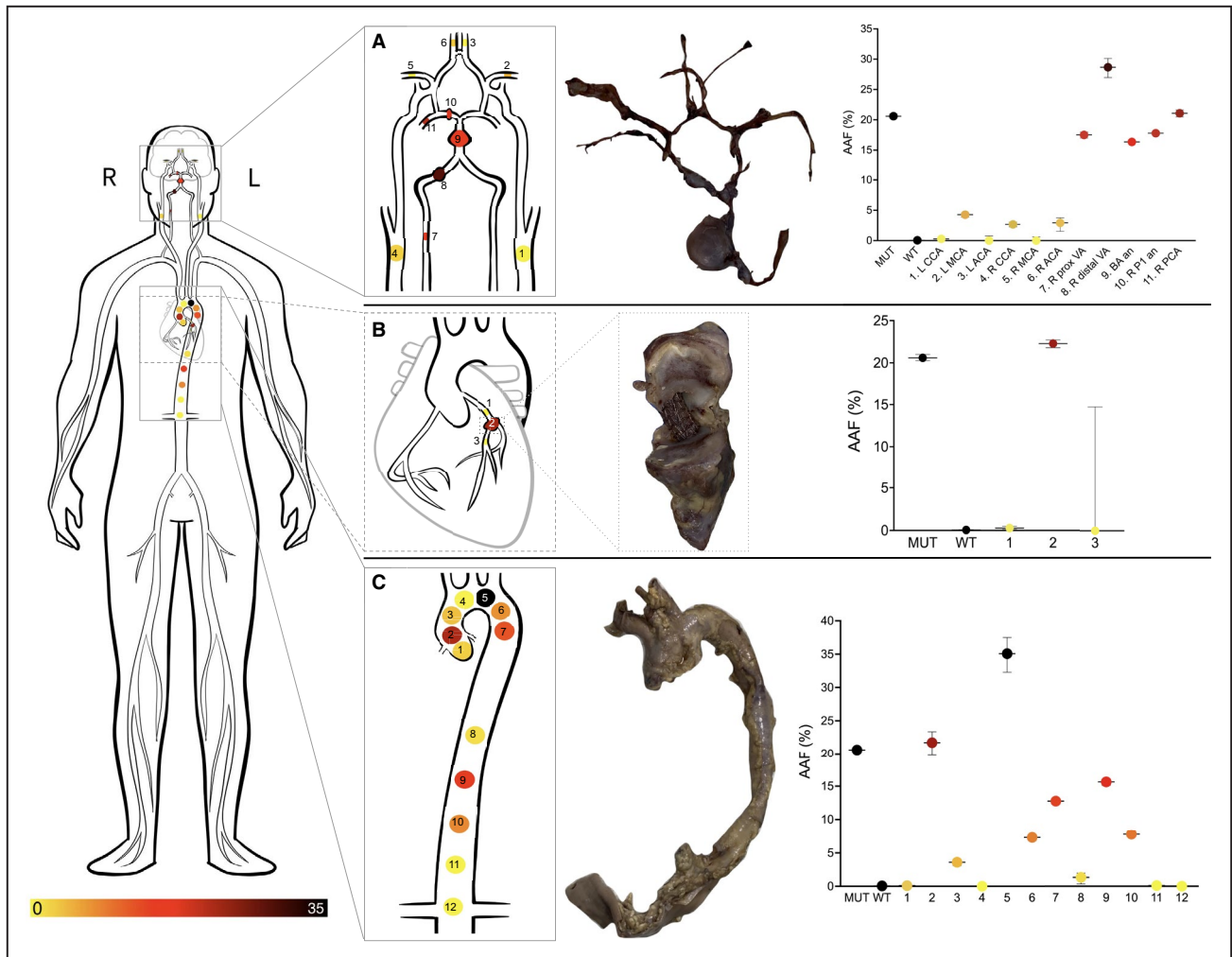


Figure 2. Heatmap of vascular samples harvested from the (A) intracranial, (B) coronary, and (C) aortic samples. Gross pathological specimens are shown as well as AAF% at the associated sampling sites.

Radial Artery

Analysis of the frozen specimens harvested from the aneurysmal radial artery revealed the presence of the *PDGFRB* variant (AAF: 20.6%). The AAF of isolated CD31+ cells was 0.05% versus 36% for isolated CD31- cells suggesting a CD31 negative, non-endothelial specific localization of the *PDGFRB* variant.

DISCUSSION

Analysis of 80 post-mortem samples from our previously published index individual reveals further evidence of mosaic expression of an activating *PDGFRB* variant and its relationship to fusiform aneurysm development. Within the cerebral vasculature specimens, the presence of the *PDGFRB* variant correlated with aneurysm phenotype (proximal and distal vertebral artery aneurysm, mid-basilar artery aneurysm, and right P1 segment aneurysm). Areas with positive, yet low AAF

(unaffected right carotid artery, right anterior cerebral artery, and left middle cerebral artery) did not have obvious aneurysmal dilation. Similarly, samples from the coronary artery revealed the presence of the *PDGFRB* variant in the aneurysmal component of the coronary artery and negative expression of the *PDGFRB* variant in the proximal and distal components of the coronary artery. Samples from the aortic arch revealed the highest AAF of all aortic samples, ranging from 21.70% to 35.07%. All other aortic specimens contained variant AAFs ranging from 0.1% to 15.8%. The patient never developed any clinically significant aortic aneurysms though early evidence of dissection was apparent on histopathologic evaluation at the areas with the highest AAF, suggesting a variable time course for the clinical phenotype of aneurysmal dilatation to develop. Finally, the *PDGFRB* variant was present in the radial artery aneurysm tissue (AAF: 20.6%).

The *PDGFRB* activating variant found in the index patient’s cerebral, coronary, and radial artery aneurysm

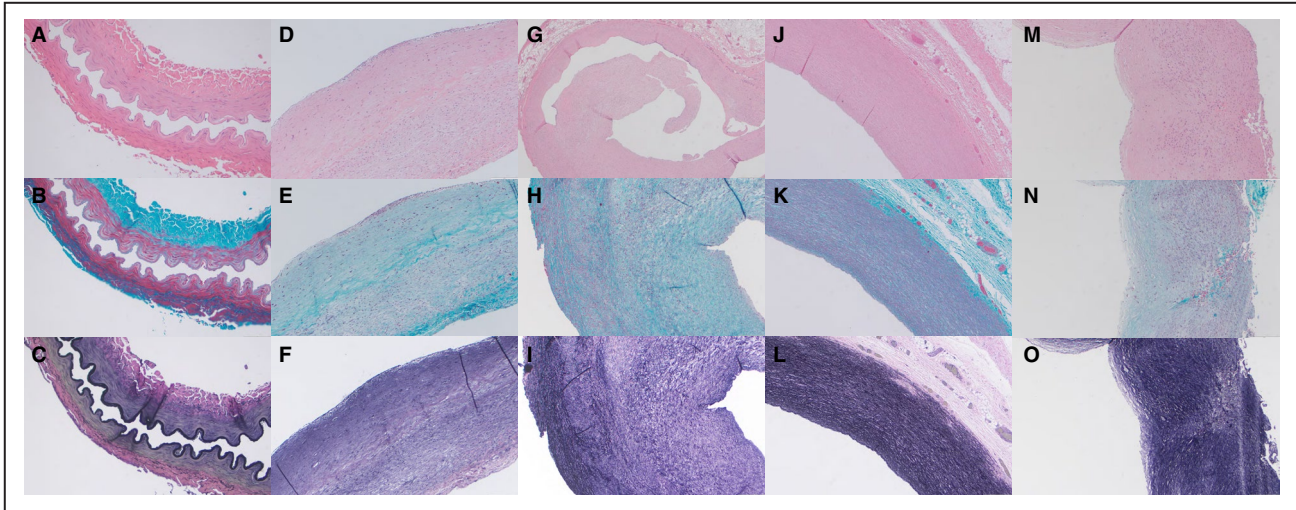


Figure 3. Histopathology of multiple vascular compartments.

Evaluation of the left anterior cerebral artery with (A) Hematoxylin and eosin (H&E) (10×) shows a well-preserved and architecturally intact cross-section of muscular artery lacking significant atheromatous change and fibrointimal hyperplasia. B, Gomori trichrome (GT) stain (10×) shows organized muscular tunica media and collagenized tunica adventitia. C, Verhoeff-van Gieson (VVG) stain (10×) shows an intact internal elastic lamina throughout the entire vessel. Histology of the ruptured mid-basilar artery aneurysm with (D) H&E (10×) shows a longitudinal section with a luminal surface variably lined by a thin layer of fibrin and reactive-appearing endothelial cells (likely related to adjacent rupture). E, GT-staining (10×) shows a proliferation of haphazardly arranged smooth muscle cells with variable nuclear pleomorphism in the tunica media. F, VVG staining (10×) highlights marked fibrointimal proliferation with extensive effacement of the internal elastic lamina. Histology of the non-aneurysmal proximal right coronary artery with (G) H&E at low power magnification (4×) shows a cross-section of muscular artery with marked fibrous intimal proliferation, a polypoid intraluminal fibrous plug and reactive endothelial changes but without significant inflammation. H, GT-stained section (10×) shows fascicular and partially disorganized proliferative tunica media with intervening collagen deposition while (I) VVG-stained tissue (10×) shows elastic fiber fragmentation and loss with effacement of the internal elastic lamina. Histology of the proximal aortic arch (Section A1) using (J) H&E (10×) shows a relatively well-preserved incomplete cross-section of elastic artery wall. K, GT staining (10×) shows focal minimal disorganization in the tunica media. L, VVG-staining (10×) shows elastic fibers admixed with smooth muscle cells in a generally uniform fashion throughout the entire tunica media except for small areas with patchy minimal degenerative changes (fragmentation of the elastica) in the tunica media. Histology of the more distal aortic arch (Section A5) with (M) H&E (10×) shows an incomplete cross-section of elastic artery wall with disordered nodular fibrointimal and medial hyperplasia. (N) GT staining (10×) shows medial hypercellularity, variable nuclear pleomorphism and architectural disorganization with intervening collagen deposition. O, VVG staining (10×) shows haphazard and patchy distribution of elastic fibers throughout the tunica media in addition to effacement of the internal elastic lamina.

tissue was absent from lymphocyte DNA and normal tissue sites, confirming it to be a non-germline somatic variant. Somatic mosaicism is one of several mechanisms for the development of cellular heterogeneity and is the natural result of the fidelity of genetic replication. Mosaicism can occur at any point following the first replication of the zygote with single nucleotide errors in DNA replication occurring at an estimated frequency of 10^{-9} errors per cellular division.^{15,16} This basal rate, alongside environmental mutagens throughout life, allow for significant genetic variation across all tissues, increasing as one ages, compared to the genome of the initial gametes. While this is a mechanism implicated in human disease, mosaicism can also lead to beneficial cellular changes in the immune system¹⁷ and development of neuronal diversity,¹⁸ enhancing the adaptive ability of tissues.¹⁹

PDGFRB encodes a transmembrane receptor tyrosine kinase involved in multiple cell signaling pathways and is critical for the growth of mesenchymal cells,

including blood vessels.¹ It is composed of four domains (1) Ig-like domain, (2) transmembrane domain, (3) juxtamembrane domain, and (4) tyrosine kinase domain. The index patient was found to have a single novel variant (p. Tyr562Cys [g.149505130T>C [GRCh37/hg19]; c.1685A>G]) within the juxtamembrane domain. In the subsequent validation cohort of non-syndromic patients with fusiform aneurysms, other variants in *PDGFRB* were identified and included a juxtamembrane domain variant predicted to result in a 4 amino acid in-frame deletion (p. Tyr562_Arg565del), and 2 additional variants (p. Asp850Tyr and p. Arg849_Lys860delinsHisAlaGly LeuGluLeuHisLeuGln) in the activation loop of the kinase domain. Furthermore, sequencing of saccular aneurysms of the validation cohort revealed only wildtype *PDGFRB* suggesting a mosaic expression associated with fusiform aneurysm formation.²

The clinical phenotype of the index patient is reminiscent of other known heritable progressive aneurysmal

pathologies including Marfan syndrome, Loeys-Dietz syndrome, and Ehlers-Danlos type IV, amongst others. These, however, show Mendelian inheritance with variable penetrance and are due to mutations in fibrillin-1, COL3A1, and TGFBR 1 and 2, respectively.²⁰ Fresh and post-mortem tissue were tested for these genetic mutations without any alterations. A notable difference in the clinical phenotype of the index patient's aneurysms, as compared to those seen in syndromic cases described above, were their fusiform appearance and presence in multiple vascular compartments. Fusiform aneurysms represent an estimated 10% of intracranial aneurysms, with histological findings of intimal layer thickening.^{20,21} The more common intracranial aneurysm variant, saccular aneurysms develop from thickened hyalinized intimal and adventitial layers with risk factors including smoking, hypertension, and a family history of saccular aneurysms. Intracranial saccular aneurysms are more readily treated via microsurgical clipping or endovascular techniques. Fusiform aneurysms, however, are significantly more difficult to treat due to the involvement of long segments of the involved vessel and poor responses to surgical clip reconstruction. While endovascular technologies have led to a revolution in the treatment of intracranial fusiform aneurysms, often a combined approach is needed, with higher surgical risks compared to the treatment of saccular aneurysms.

Since the publication of our prior study describing the association between *PDGFRB* and fusiform aneurysms, several case reports have been published describing patients with *PDGFRB* variants, due to both germline and somatic mosaicism, with dermal and/or vascular phenotypes. Chenbhanich et al reported 2 patients with the same mosaic *PDGFRB* p(Tyr562Cys) variant identified in our index patient. One 25-year-old female patient had presented with a 1-year history of progressive left eye blindness and was found to have a fusiform aneurysm of the left intracranial internal carotid artery as well as a fusiform dilation of the left anterior cerebral artery. Repeat imaging 1 year later showed interval progression of these fusiform aneurysms as well as the development of a fusiform aneurysm at the right middle cerebral artery. Whole body imaging also revealed 2 fusiform aneurysms of the coronary arteries. Targeted antibody therapy using Sorafenib, a tyrosine kinase inhibitor, was initiated, though she unfortunately experienced rupture of her left internal carotid artery aneurysm necessitating neurosurgical intervention. A second patient with the same mosaic variant was a 16-year-old female who presented with segmental hemihypertrophy of the left arm and hand and was found to have abnormal vasculature within the affected arm.¹¹ Wenger et al reported a series of 12 patients with activating *PDGFRB* mutations, with three of the older patients (ages 13, 14, and 26) found

to have aneurysms.⁹ Foster et al reported 2 patients with cerebrovascular complications including basilar artery thrombosis and aneurysmal rupture.²² Finally, Takenouchi et al retrospectively reviewed the two originally published Kosaki overgrowth syndrome patients with activating *PDGFRB* variants and discovered fusiform intracranial and coronary aneurysms.²³

Though distinct individual syndromes secondary to activating *PDGFRB* variants have been described, such as infantile myofibromatosis, Kosaki overgrowth syndrome, and Penttinen premature aging syndrome, there likely exists a phenotypic spectrum that is due to the specific activating germline or mosaic expression of the individual *PDGFRB* variant. When long-term follow-up of patients with activating *PDGFRB* variants was performed, Wenger et al proposed a 2-group classification of phenotypes termed *PDGFRB* activating disorder (PAVS) –1 and –2. PAVS-1 represents the less severe group and would include patients previously diagnosed with infantile myofibromatosis.⁹ These patients are often spared the cutaneous and skeletal morbidity of more severely affected individuals, though vascular pathology, such as aneurysms, have been reported with several affected patients dying suddenly at a young age. Specific variants, including p. Pro560Leu, p.Arg561Cys, p. Ile564_Val572del, p. Lys567Glu, and p. Pro660Thr are considered likely to lead to a less severe phenotype and subsequent designation under the PAVS-1 classification. PAVS-2 is the more severe phenotype with affected individuals presenting with multi-organ system involvement, including central nervous, musculoskeletal, skin, and vasculature systems. Phenotypes of Kosaki overgrowth syndrome, Penttinen premature aging syndrome, and multiple fusiform aneurysms seen in our index patient would be considered PAVS-2. Vascular abnormalities, including fusiform aneurysms are common with multiple reports of progressive vasculopathy as well as sudden death suggestive of aneurysmal rupture in this subclassification.^{9,10,22–24} Specific variants associated with a more severe phenotype and subsequent classification of PAVS-2 include p. Arg561_Tyr562, p. Tyr562Cys, p. Trp566Arg, p. Pro584Arg, p. Val665Ala, p. Asn666His, and p. Asn666Ser.

Ex-vivo, cell lines obtained from the index patient resulted in an increase of kinase auto-phosphorylation with subsequent phosphorylation and constitutive activation of the downstream proteins: ERK, SRC, and AKT10. This is consistent with in vitro studies of activating *PDGFRB* variants in cell lines created from patients with infantile myofibromatosis and Kosaki overgrowth syndrome.^{10,25} Notably, CD31- (non-endothelial) cells had the expressed the *PDGFRB* variant. This finding is particularly interesting as the expression of *PDGFRB* within vascular smooth muscle cells has been associated with a synthetic, rather than contractile

phenotype, resulting in increased secretion of extracellular vesicles that enhance local inflammation and promote aneurysm development.²⁶ This is consistent with histopathological findings showing varying degrees of vascular medial hyperplasia and disorganization associated with frequently marked fibrointimal hyperplasia with the most severely involved segments showing effacement of the internal elastic lamina. In addition, this differentiates fusiform aneurysms from other intracranial vascular pathology, such as arteriovenous malformations, where activating mutations are localized to the endothelial cell layer.²⁷

Tyrosine kinase inhibitors are an attractive option for the targeted treatment of pathology secondary to the constitutive activation of PDGFRB variants. Patients with infantile myofibromatosis, Penttinen-like phenotypes, and intracranial fusiform aneurysms have been treated with the tyrosine kinase inhibitors imatinib, sunitinib, and sorafenib.^{9,11,28–31} Imatinib, in combination with vinblastine, was used to treat myofibromas with a rapid and durable response in two siblings with infantile myofibromatosis.²⁸ Wenger et al reported 2 patients with severe myofibromatosis treated with imatinib with a robust response.⁹ Likewise, Pond et al reported the efficacy of imatinib in treating multiple phenotypes associated with a gain of function PDGFRB variants.²⁹ To date, however, no study has reported regression of aneurysmal phenotype following initiation of tyrosine kinase therapy. Notably, as described above, a single patient treated with sorafenib experienced intracranial aneurysm rupture 3 months following initiation of therapy.¹¹ It is unclear whether sorafenib contributed to this rupture and as such, further experimental treatments with tyrosine kinase inhibitors in patients with intracranial aneurysms should be performed with caution. Our group was in the process of discussing treatment of our index patient with a tyrosine kinase inhibitor due to profound advancement of his aneurysmal phenotype. As conventional therapeutic modalities of endovascular and open surgical repair are exhausted, systemic therapy might become an alternative. Weighing the risks and benefits and understanding the natural history is imperative prior to pursuing experimental therapies.

There were several limitations to this study. While this manuscript aims to provide a thorough characterization of the presence of the *PDGFRB* variant throughout the index individual, generalizing the results to the pathogenesis of spontaneous fusiform aneurysms requires validation in larger cohorts of both sporadic and syndromic patients. Given the rarity of presentation, future studies aimed at elucidating mechanisms of fusiform aneurysmal development would benefit from multi-institutional collaborations and tissue sharing. Second, to best identify the role of PDGFRB in aneurysm formation, in-vitro and in-vivo studies are needed to determine if downregulation of constitutive PDGFRB

phosphorylation can recover a normal vascular phenotype. Finally, there was some heterogeneity in the fixation techniques of various vascular samples given the temporal differences between tissue harvest. However, multiple groups have reported high concordance between FFPE and fresh frozen tissue in genomic assays, suggesting that differences in AAF due to fixation technique are nominal.^{32–34}

In summary, we add additional evidence showing the role of PDGFRB in the formation of intracranial and extracranial fusiform aneurysms and localize these to non-endothelial, CD31- cells. Given the significantly shortened lifespan of patients with syndromes secondary to activating *PDGFRB* variants, hypothesized to be due to ruptured aneurysms, additional therapeutic evidence for the efficacy of tyrosine kinase inhibitors in vascular remodeling are needed to decrease morbidity and prolong life.

ARTICLE INFORMATION

Received October 20, 2021; accepted January 6, 2022.

Affiliations

Departments of Neurosurgery (C.A.P., F.M.E., D.T., J.R., M.M., S.E., Y.K., T.B., A.A.N., S.M.S., M.F.), Division of Neuropathology, Department of Laboratory Medicine and Pathology (D.A.M., L.F.G.), Departments of Genome Sciences (M.O.D.), and Division of Vascular Surgery, University of Washington School of Medicine, University of Washington Medical Center, Seattle, WA (S.S.).

Acknowledgments

We thank the affected individual, his wife and mother, and referring physicians for their important contributions to this research.

Sources of Funding

This study was funded by the US National Institutes of Health under National Heart, Lung, and Blood Institute (NHLBI) grant 1R01HL103996 (to MFJ). Dr. Ferreira was supported, in part, by the Chap and Eve Alvord and Elias Alvord Chair in Neuro-Oncology in Honor of Dr. and Mrs. Ellsworth C Alvord, Jr. The funding sources had no role in the design and conduct of the study, collection, management, analysis and interpretation of the data, preparation, review or approval of the manuscript, or decision to submit the manuscript for publication.

Disclosures

None.

REFERENCES

- Andrae J, Gallini R, Betsholtz C. Role of platelet-derived growth factors in physiology and medicine. *Genes Dev*. 2008;22:1276–1312. doi: 10.1101/gad.1653708
- Karasozen Y, Osbun JW, Parada CA, Busald T, Tatman P, Gonzalez-Cuyar LF, Hale CJ, Alcantara D, O'Driscoll M, Dobyms WB, et al. Somatic PDGFRB activating variants in fusiform cerebral aneurysms. *Am J Hum Genet*. 2019;104:968–976. doi: 10.1016/j.ajhg.2019.03.014
- Thorpe J, Osei-Owusu IA, Avigdor BE, Tupler R, Pevsner J. Mosaicism in human health and disease. *Annu Rev Genet*. 2020;54:487–510. doi: 10.1146/annurev-genet-041720-093403
- Gerhardt H, Golding M, Fruttiger M, Ruhrberg C, Lundkvist A, Abramsson A, Jeltsch M, Mitchell C, Alitalo K, Shima D, et al. VEGF guides angiogenic sprouting utilizing endothelial tip cell filopodia. *J Cell Biol*. 2003;161:1163–1177. doi: 10.1083/jcb.200302047
- Hellstrom M, Kalen M, Lindahl P, Abramsson A, Betsholtz C. Role of PDGF-B and PDGFR-beta in recruitment of vascular smooth muscle cells and pericytes during embryonic blood vessel formation in the mouse. *Development*. 1999;126:3047–3055. doi: 10.1242/dev.126.14.3047

6. Johnston JJ, Sanchez-Contreras MY, Keppler-Noreuil KM, Sapp J, Crenshaw M, Finch NA, Cormier-Daire V, Rademakers R, Sybert VP, Biesecker LG. A point mutation in PDGFRB causes autosomal-dominant penttinen syndrome. *Am J Hum Genet.* 2015;97:465–474. doi: 10.1016/j.ajhg.2015.07.009
7. Takenouchi T, Okuno H, Kosaki K. Kosaki overgrowth syndrome: a newly identified entity caused by pathogenic variants in platelet-derived growth factor receptor-beta. *Am J Med Genet C Semin Med Genet.* 2019;181:650–657. doi: 10.1002/ajmg.c.31755
8. Takenouchi T, Yamaguchi Y, Tanikawa A, Kosaki R, Okano H, Kosaki K. Novel overgrowth syndrome phenotype due to recurrent de novo PDGFRB mutation. *J Pediatr.* 2015;166:483–486. doi: 10.1016/j.jpeds.2014.10.015
9. Wenger TL, Bly RA, Wu N, Albert CM, Park J, Shieh J, Chenbhanich J, Heike CL, Adam MP, Chang I, et al. Activating variants in PDGFRB result in a spectrum of disorders responsive to imatinib monotherapy. *Am J Med Genet A.* 2020;182:1576–1591. doi: 10.1002/ajmg.a.61615
10. Zarate YA, Boccutto L, Srikanth S, Pauly R, Ocal E, Balmakund T, Hinkle K, Stefans V, Schaefer GB, Collins RT II. Constitutive activation of the PI3K-AKT pathway and cardiovascular abnormalities in an individual with Kosaki overgrowth syndrome. *Am J Med Genet A.* 2019;179:1047–1052. doi: 10.1002/ajmg.a.61145
11. Chenbhanich J, Hu Y, Hetts S, Cooke D, Dowd C, Devine P, Center UCG, Russell B, Kang SHL, Chang VY, et al. Segmental overgrowth and aneurysms due to mosaic PDGFRB p. (Tyr562Cys). *Am J Med Genet A.* 2021;185:1430–1436. doi: 10.1002/ajmg.a.62126
12. Hindson BJ, Ness KD, Masquelier DA, Belgrader P, Heredia NJ, Makarewicz AJ, Bright LJ, Lucero MY, Hiddessen AL, Legler TC, et al. High-throughput droplet digital PCR system for absolute quantitation of DNA copy number. *Anal Chem.* 2011;83:8604–8610. doi: 10.1021/ac202028g
13. Luks VL, Kamitaki N, Vivero MP, Uller W, Rab R, Bovee JV, Rialon KL, Guevara CJ, Alomari AI, Greene AK, et al. Lymphatic and other vascular malformative/overgrowth disorders are caused by somatic mutations in PIK3CA. *J Pediatr.* 2015;166:1048–1054. doi: 10.1016/j.jpeds.2014.12.069
14. Piacitelli AM, Jensen DM, Brandling-Bennett H, Gray MM, Batra M, Gust J, Thaker A, Paschal C, Tsuchiya K, Pritchard CC, et al. Characterization of a severe case of PIK3CA-related overgrowth at autopsy by droplet digital polymerase chain reaction and report of PIK3CA sequencing in 22 patients. *Am J Med Genet A.* 2018;176:2301–2308. doi: 10.1002/ajmg.a.40487
15. Lynch M. Rate, molecular spectrum, and consequences of human mutation. *Proc Natl Acad Sci USA.* 2010;107:961–968. doi: 10.1073/pnas.0912629107
16. McCulloch SD, Kunkel TA. The fidelity of DNA synthesis by eukaryotic replicative and translesion synthesis polymerases. *Cell Res.* 2008;18:148–161. doi: 10.1038/cr.2008.4
17. Di Noia JM, Neuberger MS. Molecular mechanisms of antibody somatic hypermutation. *Annu Rev Biochem.* 2007;76:1–22. doi: 10.1146/annurev.biochem.76.061705.090740
18. Baillie JK, Barnett MW, Upton KR, Gerhardt DJ, Richmond TA, De Sapio F, Brennan PM, Rizzu P, Smith S, Fell M, et al. Somatic retrotransposition alters the genetic landscape of the human brain. *Nature.* 2011;479:534–537. doi: 10.1038/nature10531
19. Fernandez LC, Torres M, Real FX. Somatic mosaicism: on the road to cancer. *Nat Rev Cancer.* 2016;16:43–55. doi: 10.1038/nrc.2015.1
20. Faluk M, De Jesus O. *Saccular aneurysm.* Treasure Island (FL): Statpearls; 2021.
21. Nakatomi H, Segawa H, Kurata A, Shiokawa Y, Nagata K, Kamiyama H, Ueki K, Kirino T. Clinicopathological study of intracranial fusiform and dolichoectatic aneurysms: insight on the mechanism of growth. *Stroke.* 2000;31:896–900. doi: 10.1161/01.STR.31.4.896
22. Foster A, Chalot B, Antoniadi T, Schaefer E, Keelagher R, Ryan G, Thomas Q, Philippe C, Bruel AL, Sorlin A, et al. Kosaki overgrowth syndrome: a novel pathogenic variant in PDGFRB and expansion of the phenotype including cerebrovascular complications. *Clin Genet.* 2020;98:19–31. doi: 10.1111/cge.13752
23. Takenouchi T, Kodo K, Yamazaki F, Nakatomi H, Kosaki K. Progressive cerebral and coronary aneurysms in the original two patients with Kosaki overgrowth syndrome. *Am J Med Genet A.* 2021;185:999–1003. doi: 10.1002/ajmg.a.62027
24. Wright C, Corbally MT, Hayes R, McDermott MB. Multifocal infantile myofibromatosis and generalized fibromuscular dysplasia in a child: evidence for a common pathologic process? *Pediatr Dev Pathol.* 2020;7:385–390. doi: 10.1007/s10024-003-0107-4
25. Arts FA, Sciort R, Brichard B, Renard M, de Rocca Serra A, Dachy G, Noël LA, Velghe AI, Galant C, Debiec-Rychter M, et al. PDGFRB gain-of-function mutations in sporadic infantile myofibromatosis. *Hum Mol Genet.* 2017;26:1801–1810. doi: 10.1093/hmg/ddx081
26. Petsophonsakul P, Furmanik M, Forsythe R, Dweck M, Schurink GW, Natour E, Reutelingsperger C, Jacobs M, Mees B, Schurgers L. Role of vascular smooth muscle cell phenotypic switching and calcification in aortic aneurysm formation. *Arterioscler Thromb Vasc Biol.* 2019;39:1351–1368. doi: 10.1161/ATVBAHA.119.312787
27. Nikolaev SI, Vetiska S, Bonilla X, Boudreau E, Jauhiainen S, Rezai Jahromi B, Khyzha N, DiStefano PV, Suutarinen S, Kiehl TR, et al. Somatic activating KRAS mutations in arteriovenous malformations of the brain. *N Engl J Med.* 2018;378:250–261. doi: 10.1056/NEJMo a1709449
28. Mudry P, Slaby O, Neradil J, Soukalova J, Melicharkova K, Rohleder O, Jezova M, Seehofnerova A, Michu E, Veselska R, et al. Case report: rapid and durable response to PDGFR targeted therapy in a child with refractory multiple infantile myofibromatosis and a heterozygous germline mutation of the PDGFRB gene. *BMC Cancer.* 2017;17:119. doi: 10.1186/s12885-017-3115-x
29. Pond D, Arts FA, Mendelsohn NJ, Demoulin JB, Scharer G, Messinger Y. A patient with germ-line gain-of-function PDGFRB p. N666h mutation and marked clinical response to imatinib. *Genet Med.* 2018;20:142–150. doi: 10.1038/gim.2017.104
30. Weller JM, Keil VC, Gielen GH, Herrlinger U, Schafer N. PDGFRB mutation-associated myofibromatosis: response to targeted therapy with imatinib. *Am J Med Genet A.* 2019;179:1895–1897. doi: 10.1002/ajmg.a.61283
31. Shah DR, Dholakia S, Shah RR. Effect of tyrosine kinase inhibitors on wound healing and tissue repair: implications for surgery in cancer patients. *Drug Saf.* 2014;37:135–149. doi: 10.1007/s40264-014-0139-x
32. Oh E, Choi YL, Kwon MJ, Kim RN, Kim YJ, Song JY, Jung KS, Shin YK. Comparison of accuracy of whole-exome sequencing with formalin-fixed paraffin-embedded and fresh frozen tissue samples. *PLoS One.* 2015;10:e0144162. doi: 10.1371/journal.pone.0144162
33. Graw S, Meier R, Minn K, Bloomer C, Godwin AK, Fridley B, Vlad A, Beyerlein P, Chien J. Robust gene expression and mutation analyses of RNA-sequencing of formalin-fixed diagnostic tumor samples. *Sci Rep.* 2015;5:12335. doi: 10.1038/srep12335
34. Gao XH, Li J, Gong HF, Yu GY, Liu P, Hao LQ, Liu LJ, Bai CG, Zhang W. Comparison of fresh frozen tissue with formalin-fixed paraffin-embedded tissue for mutation analysis using a multi-gene panel in patients with colorectal cancer. *Front Oncol.* 2020;10:310. doi: 10.3389/fonc.2020.00310